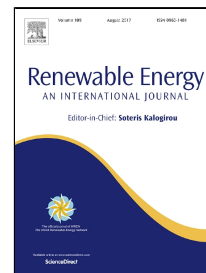


Accepted Manuscript

Synthesis of biodiesel from palm fatty acid distillate using sulfonated palm seed cake catalyst

Shehu-Ibrahim Akinfalabi, Umer Rashid, Robiah Yunus, Yun Hin Taufiq-Yap



PII: S0960-1481(17)30370-1
DOI: 10.1016/j.renene.2017.04.056
Reference: RENE 8751
To appear in: *Renewable Energy*
Received Date: 17 September 2016
Revised Date: 09 February 2017
Accepted Date: 25 April 2017

Please cite this article as: Shehu-Ibrahim Akinfalabi, Umer Rashid, Robiah Yunus, Yun Hin Taufiq-Yap, Synthesis of biodiesel from palm fatty acid distillate using sulfonated palm seed cake catalyst, *Renewable Energy* (2017), doi: 10.1016/j.renene.2017.04.056

This is a PDF file of an unedited manuscript that has been accepted for publication. As a service to our customers we are providing this early version of the manuscript. The manuscript will undergo copyediting, typesetting, and review of the resulting proof before it is published in its final form. Please note that during the production process errors may be discovered which could affect the content, and all legal disclaimers that apply to the journal pertain.

Graphical Abstract



Research Highlights

- Palm seed-based acidic catalyst was synthesized.
- Synthesized catalyst showed high acid density (12.08 mmol/g).
- 97.8% biodiesel yield was achieved at 60 °C for 2 hr reaction.
- Catalyst was successfully reused for esterification cycles (8 times) without treatment.

1 **Synthesis of biodiesel from palm fatty acid distillate using sulfonated palm seed**
2 **cake catalyst**

3
4 Shehu-Ibrahim Akinfalabi^a, Umer Rashid^{a,*}, Robiah Yunus^b, Yun Hin Taufiq-Yap^c

5
6 ^aInstitute of Advanced Technology, Universiti Putra Malaysia, 43400 UPM Serdang, Selangor,
7 Malaysia

8 ^bDepartment of Chemical and Environmental Engineering, Faculty of Engineering, Universiti
9 Putra Malaysia, 43300 UPM Serdang, Selangor, Malaysia

10 ^cCatalysis Science and Technology Research Centre, Faculty of Science, Universiti Putra
11 Malaysia, 43400 UPM Serdang, Selangor, Malaysia

12
13
14
15 *Corresponding author. Dr. Umer Rashid, Institute of Advanced Technology, Universiti Putra
16 Malaysia, 43400 UPM Serdang, Selangor, Malaysia; E-mail address: umer.rashid@yahoo.com;
17 Tel: + 60389467393; Fax: + 60389467006
18
19
20
21
22
23
24
25
26
27
28

29
30
31
32
33
34
35
36
37
38
39
40
41
42
43
44
45
46
47
48
49
50

ABSTRACT

The use of a sulfonated soaked palm seed cake (SPSC-SO₃H) derived catalyst for the production of biodiesel from palm fatty acid distillate (PFAD) (the byproduct obtained during palm oil production) has been demonstrated. The activated carbon material from the soaked palm seed cake (SPSC) was sulfonated and then used for esterification of PFAD (containing 85% of free fatty acid (FFA), 10% of triglycerides, 3% of diglycerides, 0.3% of monoglycerides and some traces of impurities). The synthesized SPSC-SO₃H catalyst was characterized using powder X-ray diffraction (XRD), Brunauer–Emmett–Teller (BET), fourier transform infrared (FTIR) spectroscopy, field emission scanning electron microscope (FESEM), NH₃-temperature programmed desorption (NH₃-TPD), N₂ physisorption and thermogravimetric analysis (TGA). The SPSC-SO₃H catalyst showed higher acid density (12.08 mmol g⁻¹) and surface area (483.07 m² g⁻¹). The optimized reaction conditions, *i.e.* 9:1 methanol/PFAD molar ratio; 60 °C reaction temperature; 2.5 wt.% of the SPSC-SO₃H catalyst and 2 h of reaction time was employed to achieve FFA conversion (98.2%) and FAME yield (97.8%). The SPSC-SO₃H catalyst underwent eight reaction cycles and catalytic activity was dropped by 24% during recyclability study. The SPSC-SO₃H catalyst demonstrates a promising and effective application for biodiesel synthesis especially for feedstocks containing high free fatty acid content.

Keywords: Palm seed cake; Palm fatty acid distillate; Heterogeneous catalyst; Sulfonation; Reusability, Biodiesel

51 1. Introduction

52 In recent years, biodiesel production as an alternative fuel source, has received more
53 attention due to the increased carbon emissions, dwindling traditional fossil resources, unstable
54 cost, and the non-renewability of petroleum fuel. Biodiesel is derived from various animal and
55 vegetable oils and it is basically comprised of a mixture of alkyl esters of fatty acids, and other
56 glycerides compounds [1]. The transesterification of vegetable oils and fats have been employed
57 to lower the viscosity levels of these fats and oils so as to meet the permissibility limit of petroleum
58 fuel [2]. Moreover, biodiesel is a clean-burning fuel because of its environmentally benign, easily
59 degradable and bio-renewable nature, good transport and storage properties, and it can be directly
60 used in modern day compression-ignition engines with no modification step needed [3].

61 Currently, different sources of vegetable oil have been used as an attractive feedstock for the
62 production of biodiesel, *i.e.* canola [4], palm [5], Jatropha [6], sunflower [7] and rapeseed [8] oils.
63 However, food grade vegetable oils have not been exploited for the production of biodiesel because
64 they will inadvertently lead to an increase in the prices of edible vegetable oils and an unhealthy
65 competition between food and fuel. Hence, there is a necessary need to explore new suitable
66 feedstock for biodiesel production. As a result, palm fatty acid distillate (PFAD), a by-product
67 from the palm oil industry has emerged as the prime candidate for biodiesel production. Of the
68 total 59 million tons of palm oil produced globally in 2014, Malaysia, being the second largest
69 global producer and exporter of palm oil, produced 19.4 million tons of palm oil which is
70 approximately 33% of the global production [9]. PFAD primarily consists of high free fatty acid
71 (FFA, 85 wt. %), triglycerides (10 wt.%) and other small contents of sterols, vitamin E and
72 squalene.

73 In industry, a base catalyst is used to convert PFAD to methyl esters, saponification usually
74 occurs, due to the high free fatty acid contents of the feedstock. In conventional esterification
75 process, homogeneous acid catalysts (H_2SO_4) are used with high quantities of alcohol, which is
76 the main factor affecting economics of biodiesel production from PFAD [10]. This also creates
77 many drawbacks *i.e.* corrosion to reactor, multiple purification steps which generates wastewater
78 and unreacted H_2SO_4 catalyst [11].

79 In other to avert this shortcoming, different types of heterogeneous solid acids such as ferric
80 hydrogen sulfate [11], ferric alginate [12], carbohydrate-derived solid acid [13], sulfonated-carbon
81 nanotubes [14], niobium-MCM-41 [15] catalysts have been investigated as viable catalysts for
82 esterification reaction. Moreover, carbon based catalysts *i.e.* sugars [13], starch [16], fiber [17],
83 resin [18], polymer [19] and glycerol [20] have also been reported. However, the expensive
84 materials, synthesis routes, low activity and reusability, reduced their industrial applicability.
85 Therefore, the development of sulfonated carbon catalysts derived from low cost biomass wastes
86 to produce biodiesel from acidic oil could be a potential and considerable interest. Palm biomass
87 accounts for about 85.5% of the total biomass generated from agricultural activities, and only about
88 10% of oil is produced, thus Malaysia has a rich source of palm biomass suitable as feedstock for
89 catalyst synthesis [9].

90 In previous study, Guldhe et al. [21] synthesized chromium-aluminum mixed oxide (CRAL)
91 heterogeneous catalyst and utilized for esterifying the PFAD. They had achieved FAME
92 conversion (98.28%) at optimum reaction conditions; reaction temperature of 80 °C, catalyst
93 concentration of 15 wt. % and 15:1 methanol-to-oil molar ratio. In another related study, rice husk-
94 derived sodium silicate was utilized for transesterification of oils at the optimal reaction
95 conditions; catalyst loading of 2.5 wt. %, methanol-to-oil molar ratio of 12:1, at 65 °C for 30 min

96 and FAME yield was 97% [22]. Similarly, the methanolysis of RBD palm oil was demonstrated
97 using calcium oxide synthesized catalyst at the following optimal conditions; 9 wt. % catalyst
98 loading, 12:1 methanol-to-oil ratio, 2 h reaction time and 60 °C and observed the conversion of
99 90.11% [23].

100 To our best knowledge, no study on the catalytic performance of sulfonated soaked palm
101 seed cake (SPSC-SO₃H) catalyst has been reported yet, for biodiesel production from PFAD. In
102 this work, the main aim was to synthesize the highly acidic palm seed cake-based catalyst and its
103 utility to generate biodiesel from PFAD. A thorough physicochemical characterization *i.e.* X-ray
104 diffraction (XRD), thermogravimetric analysis (TGA), Fourier Transform infrared (FTIR),
105 Brunauer–Emmett–Teller (BET), NH₃-temperature programmed desorption (NH₃-TPD), field
106 emission scanning electron microscope (FESEM) and carbon hydrogen nitrogen sulfur (CHNS)
107 analyses were carried out for the SPSC-SO₃H catalyst. Important reaction variables (methanol to
108 PFAD molar ratio, catalyst loading, time and temperature) were also optimized for a higher PFAD
109 conversion yield. Furthermore, the reusability study of SPSC-SO₃H catalyst was further appraised
110 to test its usability for eseterification reaction without further treatment.

111

112 2. Experimental

113 2.1. Reagents and materials

114

115 The palm seed cake and PFAD were obtained from Jomalina R&D and Sime Darby Group
116 Sdn. Bhd., Malaysia, respectively. The PFAD consists of 85 wt.% of FFA (43.2% palmitic, 30.1%
117 oleic, 7.1% linoleic, 3.6% stearic and 1.0% myristic). It also contains 10% triglycerides (TG), 3%
118 diglycerides (DG), 1% monoglycerides (MG) and some traces of impurities. Ethyl alcohol (96%),
119 methanol (99.8%), propanol (99.97%) and *n*-hexane (85%) were purchased from Merck & Co,
120 pharmaceutical company, USA. Concentrated H₂SO₄ (98%) and KOH (86%) were bought from J.

121 T. Baker. Phenolphthalein and H_3PO_4 (50%) were purchased from Sigma-Aldrich. Methyl
122 palmitate, methyl linoleate, methyl oleate, methyl heptadecanoate, methyl myristate and methyl
123 stearate were $\geq 99.0\%$ analytical grade standards purchased from Fisher Scientific and used for the
124 FAME yield determination using gas chromatography (GC). The saponification value of the crude
125 PFAD was measured using AOCS method Cd 3-25.

126
127 *2.2. Chemical activation process*

128 Two samples were prepared in order to check the progression in surface area and pore
129 volume. The first sample was measured and pyrolyzed without H_3PO_4 , whereas the other powdered
130 palm seed cake was chemically activated by soaking (20 g) with orthophosphoric acid (H_3PO_4 ;
131 50%) in the impregnation ratio of 2:1 (w/w) for 24 h at self a generated temperature to facilitate
132 high porous and specific surface area development [14]. After the soaking the PSC, the resultant
133 material was kept for calcination.

134
135 *2.3. Catalyst preparation*

136 Briefly, the palm seed cake-based acidic catalyst was synthesized using sulfonation process
137 after the pyrolysis of soaked palm seed cake. The preparation of the sulfonated solid acid catalyst
138 from the SPSC was adopted and slightly modified from the previous procedure [24]. The
139 soaked/uns soaked PSC was then transferred and calcined with tube furnace in N_2 atmosphere at
140 $400\text{ }^\circ\text{C}$ for 2 h until black material was produced. The black solid materials produced were
141 extensively washed with hot distilled/de-ionized water ($> 80\text{ }^\circ\text{C}$) until reaching $\text{pH}\sim 7$, followed
142 by drying in an oven at $80\text{ }^\circ\text{C}$ for 24 h to obtained the palm seed cake based activated carbon. After
143 drying, a mortar pestle was used to powder the PSC-AC and SPSC-AC materials. The attachment
144 of a sulfonic group ($-\text{SO}_3\text{H}$) was performed by sulfonating on the SPSC-AC (4 g) with 100 mL of

145 concentrated H_2SO_4 at $150\text{ }^\circ\text{C}$ under a nitrogen flow in a reflux system for 12 h. At the end of the
146 heating, the sample was allowed to cool down to room temperature and then slowly diluted with
147 distilled water and the black precipitate was afterwards collected. The sulfonated soaked palm seed
148 cake (SPSC- SO_3H) catalyst was then washed with hot ($> 80\text{ }^\circ\text{C}$) distilled water in order to remove
149 the possible remnants of the sulfate ions and unwanted impurities. The excess moisture was gotten
150 rid of by drying the SPSC- SO_3H catalyst in an oven for 24 h at $80\text{ }^\circ\text{C}$.

151
152 *2.4. Catalyst characterization*

153 The catalyst's structural and crystallinity were checked by X-ray diffraction (XRD). The
154 machine used for the analysis was the XRD (Shimadzu, XRD 6000) which has a scanning rate of
155 $4\text{ degrees min}^{-1}$ and a scanning range of theta (θ) from 2° to 60° . The average crystallite size of the
156 PSCW- SO_3H samples was estimated by Scherrer's formula ($D = 0.89 \lambda / \beta \text{ Cos } \theta_\beta$), where D is the
157 average crystallite size, λ is the wavelength of the X-ray beam, β is the full width half maximum
158 (FWHM) values of the peaks, and θ_β is the Bragg angle. To investigate for the thermal stability,
159 the thermogravimetric analysis (TGA) was performed with differential thermogravimetry (DTG),
160 using the Mettler Toledo 990. In order to ascertain the presence of the functional group attached
161 on the catalyst, the Fourier Transform Infrared (FTIR) from Perkin Elmer (1725 X) was deployed.
162 Prior to the surface area analysis (BET), the sample was degassed at $150\text{ }^\circ\text{C}$ and heated overnight.
163 The Sorptomatic 1990 series (Thermo Finnigan) instrument was used for the surface area
164 measurement. The acid density and active acid sites were determined by using the ammonia-
165 temperature programmed desorption (NH_3 -TPD) (Thermo Finnigan, TPDRO 1100 series) and
166 helium was used as a carrier gas. A morphological study of the samples was carried out using a
167 high magnifying field emission scanning electron microscope (FESEM) (JEOL, JSM-6400).

168

169 2.5. Catalytic activity of the SPSC-SO₃H catalyst

170 In the present study, experiments were planned to appraise the effect of different reaction
171 parameters such as methanol/PFAD molar ratio (3:1-13:1); SPSC-SO₃H catalyst loading (0.5-3.5
172 wt.%), reaction temperature (55-75 °C) and reaction time (1-6 h). The esterification reaction
173 involving the PFAD and SPSC-SO₃H catalyst in the presence of a calculated amount of alcohol, a
174 conventional reflux system was used. The 250 mL of a 2-necked flat bottom flask, containing the
175 mixture of reactants, was coupled to the condenser to re-condense the evaporated methanol back
176 into the reaction. The flask was immersed in a semi-filled silicon oil bath for the esterification
177 reaction as per scheme 1. The esterification reactions were performed by varying the amount of
178 catalyst, methanol to PFAD molar ratio, time and temperature of the reaction. Typically, 0.1g of
179 catalyst, 4 g of PFAD and 4.27 g of methanol were mixed together in the reaction system, a stirrer
180 was placed along in the flask, with a stirring speed set at 600 rpm. At the end of the reaction, the
181 reaction mixture (depending on the volume) was poured into a 50 mL centrifuge tube for
182 centrifugation at 5000 rpm for 15 min in order to ease the separation. The catalyst was further
183 washed with ethanol (30 mL at room temperature) after separation and dried at 80 °C for 4 h and
184 tested in the reuse experiments. As for the FAME, it was heated at 65 °C for 1 h to remove the
185 excess remaining methanol.

186 187 2.6. PFAD methyl ester analysis

188 According to the AOCS 5a-40 standard, the fatty acid (FA) conversions were calculated,
189 according to the differences of the free fatty acid (FFA) of the feedstock and the product [9], as
190 the following equation (Eq. 1), where; FFA_f and FFA_p represents the acid value of the feedstock
191 and the free fatty acid value of the FAME phase, respectively.

$$192 \quad \text{FFA conversion (\%)} = \frac{\text{FFA}_f - \text{FFA}_p}{\text{FFA}_f} \times 100 \quad (1)$$

193 Gas chromatography equipped with a flame ionization detector (FID) was used to analyze
 194 the FAME yield using EN 14103 method. A highly polar capillary column BPX 70, from the SGE
 195 Company (length: 60 m, ID: 0.25 mm and capillary: 0.25 mm) was used for separating the various
 196 compound compositions of the FAME. The n-hexane was used to dilute the samples. All reference
 197 standards *i.e.* methyl oleate, methyl palmitate, methyl linoleate, methyl myristate and methyl
 198 stearate were diluted to become 1000 ppm, respectively and methyl heptadecanoate was prepared
 199 as the internal standard. For a typical GC analysis injection, 1 mL of the prepared sample solution
 200 was injected into the GC injector pot. The temperature for the inlet was set at 250°C whilst the FID
 201 temperature was set at 270 °C. The GC oven's starting temperature was programmed to start at
 202 100 °C and increase to 250 °C with the temperature rate set at 10 °C min⁻¹. Eq. (2) showed the
 203 formula to calculate the FAME yield:

$$204 \quad \text{FAME yield (\%)} = \frac{\text{weight of FAME produced}}{\text{weight of theoretical FAME}} \times 100 \quad (2)$$

205 2.7. Catalyst reusability analysis

207 The reusability was carried out for the spent SPSC-SO₃H catalyst. After each esterification
 208 cycle, separation of the FAME, SPSC-SO₃H catalyst and water residue were performed. The spent
 209 catalysts were recovered from the reaction mixture and washed with ethanol to remove all possible
 210 oil residues and afterwards with hexane to remove polar and non-polar compounds from the
 211 catalyst. The SPSC-SO₃H catalyst was dried for 12 h at 80 °C and then reused for the next reaction
 212 cycle. The reusability study of SPSC-SO₃H catalyst was performed at optimized reaction
 213 parameters (*i.e.* 2.5 wt. % of the SPSC-SO₃H catalyst, reaction temperature of 60 °C, reaction time

214 of 2 h and methanol to PFAD molar ratio of 9:1) and FAME yield and FFA conversion were
215 calculated using Eq. (1) and (2). The same procedure was repeated for all the cycles.

216 217 *2.8. CHNS analysis*

218 The CHNS analysis was used to measure the amount of sulfur leached during the
219 esterification reaction. Typically, the 0.05 g of SPSC-SO₃H catalyst was collected after each run
220 and analyzed using CHNS instrument (LECO CHNS-932 spectrometer) to determine the amount
221 of leached active site (-SO₃H) from SPSC-SO₃H catalyst.

222 223 *2.9. Statistical analysis*

224 In order to analyze the data for the catalytic activities, samples were individually studied in
225 set of three as the mean \pm SD.

226 227 **3. Results and discussion**

228 *3.1. Effect of chemical activation on surface area*

229 The Brunauer–Emmett–Teller (BET) surface area analysis was carried out to investigate the
230 effect of H₃PO₄ treatment on the PSC. Two samples; the palm seed cake-activated carbon (PSC-
231 AC) and soaked palm seed cake activated carbon (SPSC-AC) were analyzed for nitrogen
232 adsorption/desorption measurements and results are summarized in Table 1. The SPSC-AC
233 showed a type 4 mesoporous structure with H4 hysteresis loop which is a typical feature of a slip-
234 shaped pore which clearly defines a mesoporous material. On the other hand the PSC showed a
235 type 1 structure which is a main feature of a microporous material [19]. Based on the nitrogen
236 quantity adsorbed at different relative pressures, the specific surface area of the PSC-AC (107 m²
237 g⁻¹) and the SPSC-AC (658 m² g⁻¹) was calculated by the Brunauer–Emmett–Teller (BET) method.
238 The recorded pore diameter for the SPSC-AC was 5.09 nm and pore volume of 1.18 cm³ g⁻¹,

239 whereas the PSC-AC pore diameter and pore volume was 0.95 nm and 0.15 cm³ g⁻¹, respectively.
240 Therefore, there was an apparent increment in the specific surface area, pore volume and pore
241 diameter of the SPSC-AC as depicted in Table 1. These results indicate that H₃PO₄ is an effective
242 activating agent that promotes the development of porosity and can help to increase the surface
243 area to a reasonable margin [25-26].

244 3.2. Characterization of the SPSC-SO₃H catalyst

246 3.2.1. XRD analysis

247 The x-ray diffraction patterns (Fig 1), confirms the amorphous nature of PSC, SPSC-AC and
248 SPSC-SO₃H catalyst. They all revealed weak but broad diffraction peaks of (002) and (101) at 2θ
249 values ranged from 10-30° and 38-45°, respectively, which is attributed to the amorphous carbon
250 natures composed of aromatic carbon sheets oriented in a relatively random manner in the
251 carbonaceous materials [16, 27]. The bio-based material becomes completely black which might
252 be indication of dehydration process to form polyaromatic/carbon on the surface [27], whereas,
253 the sharp peaks may indicate the presence of inorganic substances [28].

254 3.2.2. FT-IR analysis

256 The FTIR spectra of typical absorption signals observed from Fig 2 shows band recorded at
257 1118 cm⁻¹ which confirms the presence of the sulfonic group (-SO₃H), covalently bonded to
258 polyaromatic carbon structure on the SPSC-SO₃H catalyst. The stretching bands at range of 1500-
259 1700 cm⁻¹ for both the SPSC-AC (Fig. 2b) and SPSC-SO₃H catalyst (Fig. 2c) was indication for
260 typical carbonyl functional groups (C=O); which is characteristic peaks of incompletely
261 carbonized carbons [29]. Other stretching band that appeared at 1180 (P=O stretching), indicated
262 the incorporation of H₃PO₄ as an acid activation agent on the non-sulfonated carbon surfaces of
263 the PSC-AC (Fig. 2b) [29].

264

265 *3.2.3. FESEM and EDX analysis*

266 Fig. 3 shows the FESEM images of the PSC, SPSC-AC and SPSC-SO₃H catalyst. All the
267 materials exhibited aggregate and irregular particles. The surface texture of the PSC changed
268 significantly after soaking with H₃PO₄ and sulfonation with H₂SO₄. Upon the H₃PO₄ acid
269 treatment of PSC (Fig. 3b) and sulfonation of SPSC-AC (Fig. 3c), the porosity of the carbon
270 materials, increased in arrangement of PSC < SPSC-AC < SPSC-SO₃H catalyst, respectively, as
271 clearly seen in the FESEM images (Fig. 3). The EDX and CHNS analysis (Table 2) data clearly
272 depicts that the predominantly the carbon, hydrogen and sulfur in all the materials. The existing of
273 sulfur in SPSC-SO₃H catalyst was proved to confirm the sulfonation of the -SO₃H functional group
274 on the surface of the catalyst.

275

276 *3.2.4. NH₃-TPD analysis*

277 The total amount of acidity and active acid site distributions were determined by the NH₃-
278 TPD analysis. The NH₃ desorption profiles of PSC, SPSC-AC, and SPSC-SO₃H catalyst are
279 depicted in Fig 4 and the amount of acidity of the SPSC-SO₃H catalyst is summarized in Table 2.
280 For PSC (Fig. 4a), the appearance of two broader desorption peaks were observed as weakly and
281 moderately of acid sites which may be due to the interaction between -NH₃ and residue of the
282 unreacted carbon sheets [30]. The NH₃-TPD profile of the SPSC-AC (Fig. 4b) exhibited the NH₃
283 desorption peaks in ranges of 100-300 °C and 400-700 °C after the chemical activation process
284 with H₃PO₄ acid. This indicated that a Lewis acid site and a Brønsted acid site were found at the
285 desorption peak with T_{\max} of 180 °C and 630 °C [31], respectively. The SPSC-SO₃H catalyst (Fig.
286 4c) showed strong acid sites desorption peak at the T_{\max} of 780 °C after sulfonation, but it also
287 showed a relatively lower weak acid sites at the T_{\max} of 210 °C. Moreover, SPSC-SO₃H catalyst

288 has also demonstrated a moderately desorption peak at the T_{\max} of 550 °C. Similar sulfonation
289 peaks were reported by Lokman et al. [32] for sugar based solid acid catalyst.

290
291 *3.2.5. Thermo-gravimetric analysis*

292 The thermal stability of the PSC, SPSC-AC and SPSC-SO₃H catalyst were tested with the
293 thermo-gravimetric analysis (TGA) under a nitrogen flow. As expressed in Fig. 5, each of the
294 samples had an initial weight water loss at around 100 °C from the samples. Firstly, the PSC was
295 underwent for early weight loss occurring around 220-400 °C where it maintained thermal stability
296 before losing the weight. The H₃PO₄ treatment changed the pattern of thermal decomposition due
297 to which SPSC-AC showed a better stability than PSC. The SPSC-SO₃H catalyst demonstrated a
298 very excellent thermal stability under inert atmosphere. The weight loss of water occurred in the
299 region of 0-100 °C, followed by a steady and gradual loss of weight until 420 °C which could be
300 due to the decomposition of the -SO₃H acid group from the SPSC-SO₃H catalyst. It was thermally
301 stable at temperature close to 300 °C before start the decomposition of the -SO₃H group but from
302 420-800 °C there was gradual and steady weight loss. The thermal decomposition reported
303 elsewhere for carbon-based solid acid catalysts is similar to our synthesized bio-based acid catalyst
304 [33].

305
306 *3.2.6. BET surface area analysis*

307 The BET surface area analysis of PSC, SPSC-AC and SPSC-SO₃H catalyst were analyzed
308 with the relevant nitrogen adsorption/desorption isotherms, and the results are summarized in
309 Table 1. Based on the nitrogen quantity adsorbed at different relative pressures, the surface area
310 was calculated by BET analysis. SPSC-AC (658.34 m² g⁻¹) had the highest surface area compared
311 to SPSC-SO₃H (483.07 m² g⁻¹) and PSC (89.41 m² g⁻¹) and this was clearly as a result of the
312 soaking of the PSC in H₃PO₄. This result also indicates that the presence of -SO₃H acid functional

313 group had a mild effect on the surface area of SPSC-SO₃H catalyst, which may be due to the partial
314 disturbance of the surface area during sulfonation [17, 34]. The surface area of SPSC-SO₃H
315 catalyst (483.07 m² g⁻¹) was a bit lower than the surface area of the Mesua-derived activated carbon
316 sulphonate (MAC- SO₃H) (556 m² g⁻¹) [30].

317

318 3.3. Chemical properties of crude PFAD

319 The free fatty acid (FFA) and saponification value of the crude PFAD was determined
320 using the AOCS methods. The FFA content of the PFAD was 85.01 mg KOH/mg of PFAD and
321 the saponification value was 232.8 mg KOH/g, respectively. The fatty acids components were
322 analyzed with GC-FID and it consists of 43.2% palmitic, 30.1% oleic, 7.1% linoleic, 3.6% stearic
323 and 1.0% myristic. It was also contains 10% triglycerides (TG), 3% diglycerides (DG), 1%
324 monoglycerides (MG) and some traces of impurities.

325

326 3.4. PFAD esterification process

327 3.4.1. Effect of methanol/PFAD molar ratio on FFA conversion

328 An important variable in ensuring a complete reaction that involves the conversion of FFA,
329 is the amount of alcohol utilized. In this case, methanol was used in various molar ratios, ranging
330 from 3:1 to 13:1 as presented in Fig 6a. During the esterification reaction, the following reaction
331 conditions were maintained *i.e.* reaction time 2h, reaction temperature 60 °C, and 2 wt. % of the
332 SPSC-SO₃H catalyst. Fig 6a clearly shows that as the methanol-to-PFAD molar ratio increased the
333 FFA conversion also increased. At 9:1 methanol-to-PFAD molar ratio, the highest FFA conversion
334 of 87.7% was achieved. More methanol was added to further increase the methanol-to-PFAD
335 molar ratio to check for possible increments in the FFA conversion, from 11:1 and 13:1, but the
336 FFA conversion reduced to 84.4 and 84.3 %, respectively. This lack of a significant increase in the
337 FFA conversion can be attributed to the fact that excess water may produced during the

338 esterification reaction, which thus reacted with the PFAD and, therefore pushed the reaction
339 backwards. Although, in principle, an abundant amount of methanol is needed to push the reaction
340 to the product side since esterification is a reversible reaction but this principle was not effective
341 [26-30]. As a result, the 9:1 methanol-to-PFAD molar ratio was chosen as an optimum condition
342 for further study. Zhang and Jiang [35], utilized methanol-to-oil molar ratio of 24:1 in the
343 esterification of *Zanthoxylum bungeanum* seed oil. Whereas, Guldhe et al. optimized 15:1
344 methanol-to-oil molar ratio to achieved the conversion upto 98.28% [21]. This clearly shows that
345 in the present study less molar ratio of methanol to PFAD was used as compared to other published
346 work.

347 348 3.4.2. Effect of the SPSC-SO₃H catalyst dosage on FFA conversion

349 Fig 6b shows the SPSC-SO₃H catalyst ranges from 0.5 to 3.5 wt.% for the conversion of the
350 FFA. As expected, there was an increase in the FFA conversion as the weight percentage of the
351 catalyst increased. The conversion steadily increased as the amount of catalyst increased until it
352 reached 3 wt. %, where the FFA conversion rose up to 92.1 % before it reduced to 90 % at 3.5 wt.
353 %. The starting conversion of 49.6 % when 0.5 wt. % of SPSC-SO₃H was used, showed a 42.5 %
354 conversion difference when the catalyst weight was increased to 3 wt. %. There was an observed
355 reduction in the conversion when 3.5 wt. % was applied, which indicated that though a sufficient
356 amount of catalyst was needed for the optimum conversion, an excess of the catalyst would not
357 have increased the FFA conversion. This was because there was more than enough mass transfer
358 or contact rate between the catalyst and the methanol, and the feedstock had already reached the
359 equilibrium point [36]. It is as a result of this, that 2.5 wt. % was chosen for further optimization
360 studies as the optimum catalyst concentration. Other operating conditions that were kept constant
361 during the reaction are: reaction time 2h, methanol-to-PFAD molar ratio 9:1, and reaction

362 temperature 60 °C. Acidified soybean soap stock for biodiesel was used by Guo et al [37], for the
363 production of biodiesel using the lignin-derived carbonaceous solid acid catalyst. In their work, an
364 excess of 7 wt. % of their synthesized catalyst was used to convert the FFA up to 96 %.

365
366 *3.4.3. Effect of reaction temperature on FFA conversion*

367 The role of temperature was studied in the FFA conversion by varying the temperatures from
368 55 to 75 °C; whilst the following parameters were kept constant all through the reactions; reaction
369 time 2 h, catalyst loading 2.5 wt. % and 9:1 methanol-to-PFAD molar ratio. Activation energy was
370 needed to ensure protonation of the FFA conversion, since the esterification reaction is an
371 exothermic reaction [38]. An increased temperature, as expected, increased the esterification rates.
372 At 60 °C, a 98.5 % FFA conversion was observed as seen in Fig 6c, which shows the highest FFA
373 conversion rate. Although the temperature was further increased to 75 °C, but there was no
374 significant FFA conversion. Hence, 60 °C was chosen as the optimum temperature for further
375 studies. In a similar work done by Leung and Guo [39] and also by Hayyan et al. [40] all showed
376 that higher temperatures above 50 and 60 °C, respectively, directly affect the FFA conversions.
377 Guldhe et al. also optimized the biodiesel yield and achieved 98.28% conversion at 80 °C of
378 reaction temperature [21].

379
380 *3.4.4. Effect of reaction time on FFA conversion*

381 Under a continuous methanol single-pot system the effect of the reaction time was
382 investigated and the results have been presented in Fig 6d. Enough contact time was required for
383 all the media involved, for there to be the optimum FFA conversion. During the optimization of
384 reaction time, the optimized reaction conditions; 60 °C of reaction temperature, 9:1 methanol-to-
385 PFAD molar ratio and 2.5 wt. % of SPSC-SO₃H catalyst concentration was kept constant. Different
386 reaction times from 1 to 6 h were observed. The FFA conversion progressed smoothly as the

387 reaction time increased, but early on in the first h to 6 h reaction time, the FFA conversion
388 maintained a steady conversion rate that was above 82 % in the first h and 91 % in the 6 h, although
389 the best FFA conversion was recorded in the second hour with a conversion rate of 97.2 %. It is
390 imperative, therefore, to save energy and to reduce any further reaction time since the transfer rates
391 add no significance in the overall FFA conversion. Dekkhoda et al. [41], produced biochar based
392 solid acid catalyst for biodiesel production and optimized 3 h reaction time. In our present study,
393 we had achieved better reaction time as compared to other published studies [36].

394 3.5. Yield of the PFAD methyl esters at optimum conditions

396 The FAME yield (97.8 %) was obtained at following optimized reaction conditions: reaction
397 time of 2 h, reaction temperature of 60 °C, 9:1 methanol to PFAD molar ratio and 2.5 wt. % of the
398 SPSC-SO₃H. The predominant ester was methyl palmitate (42.9%), followed by methyl oleate
399 (29.6%), then methyl linoleate (7.0%), methyl stearate (3.5%), and finally methyl myristate
400 (0.9%).

401 3.6. Catalyst deactivation and reusability analysis

403 One of the major critical advantages of using the heterogeneous solid acid catalyst is its
404 reusability. A catalyst that has more reusable cycles without reactivation is regarded as more stable.
405 In order to check for the reusability, the CHNS analysis (Table 2) was performed on each of the
406 SPSC-SO₃H catalyst recovered after the esterification reaction. The result has been presented in
407 Fig 8, where the catalyst was able to go up to 8 cycles having a final FAME yield of 68.2 % and
408 FFA conversion of 69.8 % at optimum reaction conditions as presented in Fig 7. In a related work
409 by Alhassan et al. [11] where they used hydrogen sulphate as a heterogeneous solid acid catalyst
410 to produce biodiesel, they were only able to reuse their catalyst for five cycles and similarly,
411 Guldhe et al. [21] also reused the sulfonated catalyst for four catalytic batches.

412

413 **4. Conclusions**

414 The synthesis of sulfonated soaked palm seed cake has been demonstrated for the production
415 of biodiesel. In this study, SPSC-SO₃H catalyst has been efficiently used for highly acidic PFAD,
416 which contained around 85 wt.% of FFA, for biodiesel production. The synthesized SPSC-SO₃H
417 catalyst showed good thermal stability, better acid density, sufficient porosity and reusability. The
418 SPSC-SO₃H catalyst illustrated the high catalytic activity during esterification reaction. The
419 attached sulfonic group largely affected the FFA conversion rates as compared to PSC and SPSC-
420 AC. The FFA conversion of 98.2 % and the FAME yield of 97.8% were achieved under the
421 optimized reaction conditions of 9:1 methanol-PFAD molar ratio, 2 h reaction time, 60 °C reaction
422 temperature and 2.5 wt. % of SPSC-SO₃H catalyst loading. The SPSC-SO₃H catalyst was
423 successfully reused for esterification cycles (8 times) due to the stable attachment of the –SO₃H
424 functional group. Moreover, the leached sulfur content was insignificant for the first five reaction
425 runs, but it gradually decreases across the sixth through the eighth runs. In this study, the SPSC-
426 SO₃H catalyst maintained good reusability and better catalyst activity for PFAD to produce higher
427 biodiesel yield, which indicated that some other waste biomass could be utilized to produce
428 efficient solid acid catalyst for waste oils.

429

430

431 **Acknowledgement**

432 The authors wish to acknowledge the financial support from The World Academy of Sciences
433 (TWAS), Italy through Project No. 13-285 RG/REN/AS_C.

434

435 **References**

436 [1] F. Ma, M.A. Hanna, Biodiesel production: a review. *Bioresour Technol* 70 (1999) 1–15.

- 437 [2] A. Demirbas. Biodiesel production via non-catalytic SCF method and biodiesel fuel
438 characteristics. *Energ Convers Manage* 47 (2006) 2271–2282.
- 439 [3] DYC. Leung, X. Wu, MKH. Leung. A review on biodiesel production using catalyzed
440 transesterification. *Appl Energ* 87 (2010) 1083–1095.
- 441 [4] MG. Kulkarni, AK. Dalai, NN. Bakhshi. Transesterification of canola oil in mixed
442 ethanol/methanol system and use of esters as lubricative additive. *Bioresour Technol.* 98
443 (2007) 2027–2033.
- 444 [5] ZIZ. Lubes, M. Zakaria. Analysis of parameters for fatty acid methyl esters production from
445 refined palm oil for use as biodiesel in the single- and two stage processes. *Malaysian J*
446 *Biochem Mol Biol* 17 (2009) 5-9.
- 447 [6] YH. Taufiq-Yap, HV. Lee, MZ. Hussein, R. Yunus. Calcium-based mixed oxide catalysts for
448 methanolysis of *Jatropha Curcas* oil to biodiesel. *Biomass Bioenerg.* 35 (2011) 827-834.
- 449 [7] U. Rashid, F. Anwar, BR. Moser, S. Ashraf. Production of sunflower oil methyl esters by
450 optimized alkali-catalyzed methanolysis. *Biomass Bioenerg* 32 (2008) 1202-1205.
- 451 [8] JCA. Gaya, MK. Patel. Biodiesel from rapeseed oil and used frying oil. In: European Union;
452 Technical Report by Copernicus Institute for Sustainable Development and Innovation,
453 Utrecht University: Utrecht, The Netherlands, 2003.
- 454 [9] Malaysian Palm Oil Board. 2016. www.mpob.gov.my
- 455 [10] S. Chongkhong, C. Tongurai, P. Chetpattananodh, C. Bunyakan. Biodiesel production by
456 esterification of palm fatty acid distillate. *Biomass Bioenerg* 31 (2007) 563-568.
- 457 [11] F.H. Alhassan, R. Yunus, U. Rashid, K. Sirat, A. Islam, HV. Lee. Production of biodiesel
458 from mixed waste vegetable oils using ferric hydrogen sulphate as an effective reusable
459 heterogeneous solid acid catalyst. *Appl Catal A-Gen* 456 (2013) 182-187.
- 460 [12] P.L. Boey, S. Ganesan, GP. Maniam, M. Khairuddean. Sequential conversion of high free
461 fatty acid oils into biodiesel using a new catalyst system. *Energ* 46 (2012) 132-139.
- 462 [13] G. Chen, B. Fang. Preparation of solid acid catalyst from glucose-starch mixture for biodiesel
463 production. *Bioresour Technol* 102 (2011) 2635-2640.
- 464 [14] S.H. Shuit, SH. Tan. Feasibility study of various sulphonation methods for transforming
465 carbon nanotubes into catalysts for the esterification of palm fatty acid distillate. *Energ Conver*
466 *Manag* 88 (2014) 1283–1289

- 467 [15] C. García-Sancho, R. Moreno-Tost, JM. Merida-Robles, J. Santamaría-Gonzalez, A. Jimenez-
468 Lopez, P. Maireles-Torres. Niobium-containing MCM-41 silica catalysts for biodiesel
469 production. *Appl Catal B-Environ* 108 (2011) 161-167.
- 470 [16] V. Budarin, JH. Clark, JJE. Hardy, R. Luque, K. Milkowski, SJ. Tavener, AJ. Wilson.
471 Starbons: New starch-derived mesoporous carbonaceous materials with tunable properties.
472 *Angewandte Chemie International Edition*, 45 (2006) 3782–3786.
- 473 [17] Z. Fu, H. Wan, X. Hu, Q. Cui, G. Guan. Preparation and catalytic performance of a carbon-
474 based solid acid catalyst with high specific surface area. *React Kin Mech Cat* 107 (2012) 203–
475 213.
- 476 [18] B. Chang, J. Fu, Y. Tian, X. Dong. Soft-template synthesis of sulfonated mesoporous carbon
477 with high catalytic activity for biodiesel production. *RSC Advances* 3 (2013) 1987–1294.
- 478 [19] P. Xia, FJ. Liu, C. Wang, SF. Zuo, CZ. Qi. Efficient mesoporous polymer based solid acid
479 with superior catalytic activities towards transesterification to biodiesel. *Catal Commun* 26
480 (2012) 140–143.
- 481 [20] BLAP. Devi. KN. Gangadhar, PSS. Prasad, B. Jagannadh, RBN. Prasad. A glycerol-based
482 carbon catalyst for the preparation of biodiesel *Chem-SusChem* 2(7) (2009) 617–620.
- 483 [21] A. Guldhe, CV. Moura, P. Singh, I. Rawat, EM. Moura, Y. Sharma, F. Bux. Conversion of
484 microalgal lipids to biodiesel using chromium-aluminum mixed oxide as a heterogeneous
485 solid acid catalyst. *Renew. Energ.* 105 (2017) 175-182.
- 486 [22] W. Roschat, T. Siritanon, B. Yoosuk, V. Promarak. Rice husk-derived sodium silicate as a
487 highly efficient and low-cost basic heterogeneous catalyst for biodiesel production. *Energ.*
488 *Conver. Manag.* 119 (2016) 453-462.
- 489 [23] BK. Uprety, W. Chaiwong, C. Ewelike, S.K. Rakshit. Biodiesel production using
490 heterogeneous catalysts including wood ash and the importance of enhancing byproduct
491 glycerol purity. *Energ. Conver. Manag.* 115 (2016) 191-199.
- 492 [24] F. Ezebor, M. Khairuddean, AZ. Abdullah, PL. Boey. Esterification of oily-FFA and
493 transesterification of high FFA waste oils using novel palm trunk and bagasse-derived
494 catalysts *Energ Conver Manag* 88 (2014) 1143–1150.

- 495 [25] W. Youyu, F. Zaihui, Y. Dulin, X. Qiong, L. Fenglan, L. Chunli, M. Liqu. Microwave-
496 assisted hydrolysis of crystalline cellulose catalyzed by biomass char sulfonic acids. Green
497 Chem. 12 (2010) 696.
- 498 [26] J.J. Kingsley, K. Suresh, K.C. Patil. Combustion synthesis of fine-particle metal aluminates.
499 Mater Sci 25 (1990) 1305.
- 500 [27] S. Cimino, L. Lisi, S.D. Rossi, M. Faticanti, P. Porta. Methane combustion and CO oxidation
501 on LaAl_{1-x}Mn_xO₃ perovskite-type oxide solid solutions Appl. Catal., B: Environ 43 (2003)
502 397.
- 503 [28] T. Verneresson, P.R. Bonelli, E.G. Cerrella, A.L. Culierman. Arundo donax cane as a precursor
504 for activated carbons preparation by phosphoric acid activation. Bioresour. Technol. 83 (2002)
505 95-104.
- 506 [29] M. Okamura, A. Takagaki, M. Toda, J.N. Kondo, K. Domen, T. Tatsumi, M. Hara, S. Hayashi.
507 Acid-catalyzed reactions on flexible polycyclic aromatic carbon in amorphous carbon. Chem.
508 Mater 18 (2006) 3039.
- 509 [30] L.J. Konwar, R. Das, A.J. Thakur, E. Salminen, P. Mäki-Arvelac, N. Kumarc, J-P. Mikkolac,
510 D. Deka. Biodiesel production from acid oils using sulfonated carbon catalyst derived from
511 oil-cake waste. J Mol Catal A: Chem 388–389 (2014) 167–176
- 512 [31] F.A. Dawodu, O. Ayodele, J. Xin, S. Zhang, D. Yan. Effective conversion of nonedible oil
513 with high free fatty acid into biodiesel by sulphonated carbon catalyst. Appl Energy 114
514 (2014) 819.
- 515 [32] I.M. Lokman, U. Rashid, Y.H. Taufiq-Yap, R. Yunus. Methyl ester production from palm
516 fatty acid distillate using sulfonated glucose-derived acid catalyst Renew Energ 81 (2015)
517 347-354.
- 518 [33] J.R. Kastner, J. Miller, D.P. Geller, J. Locklin, L.H. Keith, T. Johnson. Catalytic esterification
519 of fatty acids using solid acid catalysts generated from biochar and activated carbon. Catal
520 Today 190 (2012) 122-132
- 521 [34] S. Soltani, U. Rashid, R. Yunus, Y.H. Taufiq-Yap. Biodiesel production in the presence of
522 sulfonated mesoporous ZnAl₂O₄ catalyst via esterification of palm fatty acid distillate
523 (PFAD). Fuel 178 (2016) 253-262.

- 524 [35] J. Zhang, L. Jiang. Acid-catalyzed esterification of *Zanthoxylum bungeanum* seed oil with
525 high free fatty acids for biodiesel production. *Bioresour Technol*, 99 (2008) 8995-9008.
- 526 [36] D. Yujaroen, G. Motonobu, M. Sasaki, A. Shotipruk. Esterification of palm fatty acid
527 distilled (PFAD) in supercritical methanol: effect of hydrolysis on reaction reactivity. *Fuel*
528 88 (2009) 2011-2016.
- 529 [37] F. Guo, ZL. Xiu, ZX. Liang. Synthesis of biodiesel from acidified soybean soap stock using
530 a lignin-derived carbonaceous catalyst. *Appl Energ* 98 (2012) 47-52.
- 531 [38] T. Liu, Z. Li, W. Li, C. Shi, Y. Wang. Preparation and characterization of biomass carbon-
532 based solid acid catalyst for the esterification of oleic acid with methanol. *Bioresour Technol*
533 133 (2013) 618-621.
- 534 [39] DYC. Leung, Y Guo. Transesterification of neat and used frying oil: optimization for
535 biodiesel production. *Fuel Process Technol* 87 (2006) 883-890.
- 536 [40] A. Hayyan, MZ. Alam, MES. Mirghani, NA. Kabbashi, NINM. Hakimi, YM Siran. Reduction
537 of high content of free fatty acid in sludge palm oil via acid catalyst for biodiesel production.
538 *Fuel Process Technol* 92 (2011) 920-924.
- 539 [41] AM. Dehkoda, AH. West, N. Ellis. Biochar based solid acid catalyst for biodiesel
540 production. *Appl Catal A-Gen* 382 (2010) 197-204.

541
542
543

544 **Figure captures:**

545 **Fig. 1** XRD patterns of (a) palm seed cake (PSC) (b) soaked palm seed cake – activated carbon
546 (SPSC-AC) and (c) sulphonated soaked palm seed cake (SPSC-SO₃H) catalyst

547 **Fig. 2** FT-IR spectra of (a) palm seed cake (PSC) (b) soaked palm seed cake – activated carbon
548 (SPSC-AC) and (c) sulphonated soaked palm seed cake (SPSC-SO₃H) catalyst

549 **Fig. 3** FESEM images of (a) palm seed cake (PSC) (b) soaked palm seed cake – activated carbon
550 (SPSC-AC) and (c) sulphonated soaked palm seed cake (SPSC-SO₃H) catalyst

551 **Fig. 4** NH₃-TPD of (a) palm seed cake (PSC) (b) soaked palm seed cake – activated carbon (SPSC-
552 AC) and (c) sulphonated soaked palm seed cake (SPSC-SO₃H) catalyst

553 **Fig. 5** Depiction of TGA analysis of (a) palm seed cake (PSC) (b) soaked palm seed cake –
554 activated carbon (SPSC-AC) and (c) sulphonated soaked palm seed cake (SPSC-SO₃H) catalyst

555 **Fig. 6** Optimized reaction parameters; (a) methanol-to-PFAD molar ratio; (b) SPSC-SO₃H catalyst
556 concentration (c) reaction temperature; and (d) reaction time for conversion of FFA from PFAD.

557 **Fig. 7** FFA conversion, FAME yield and leached sulfur ion during reusability study at optimized
558 reaction conditions: reaction time = 2 h, reaction temperature = 60 °C, methanol-to-PFAD molar
559 ratio = 9:1 and catalyst loading = 2.5wt. %.

560 **Scheme 1** Experimental set up diagram for esterification reaction.

561

562

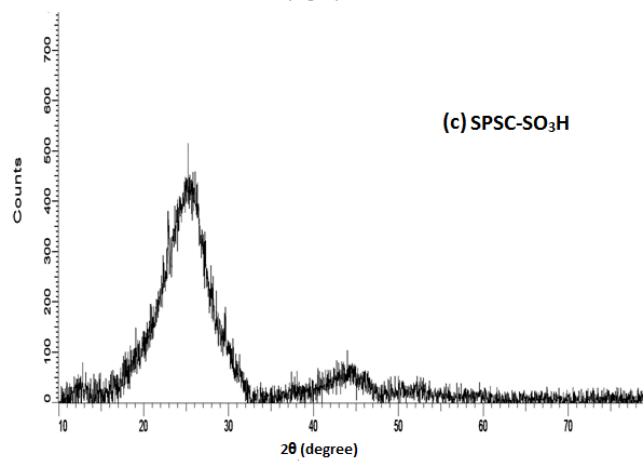
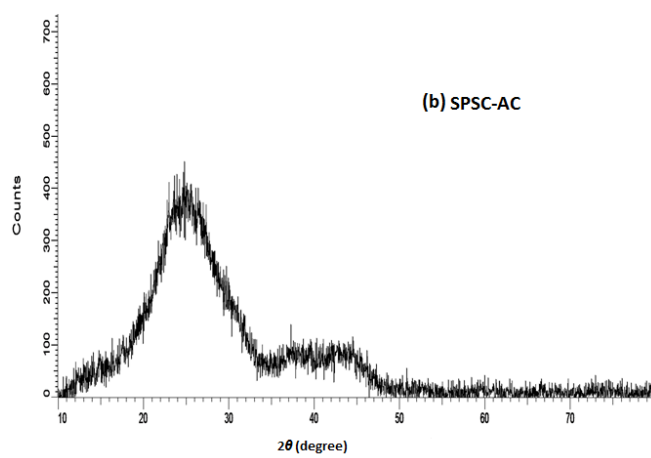
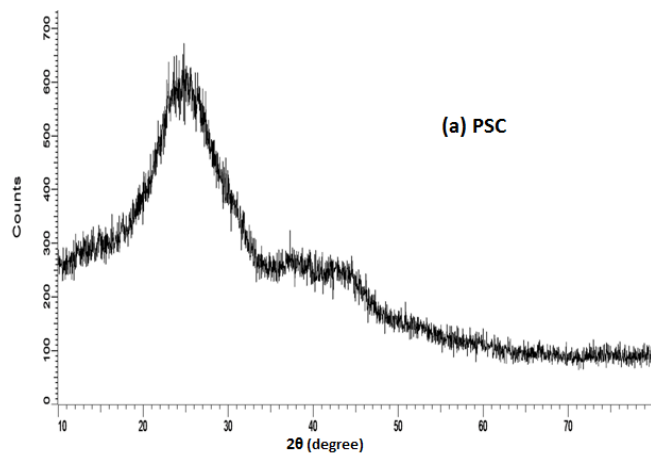
563

564

565

566

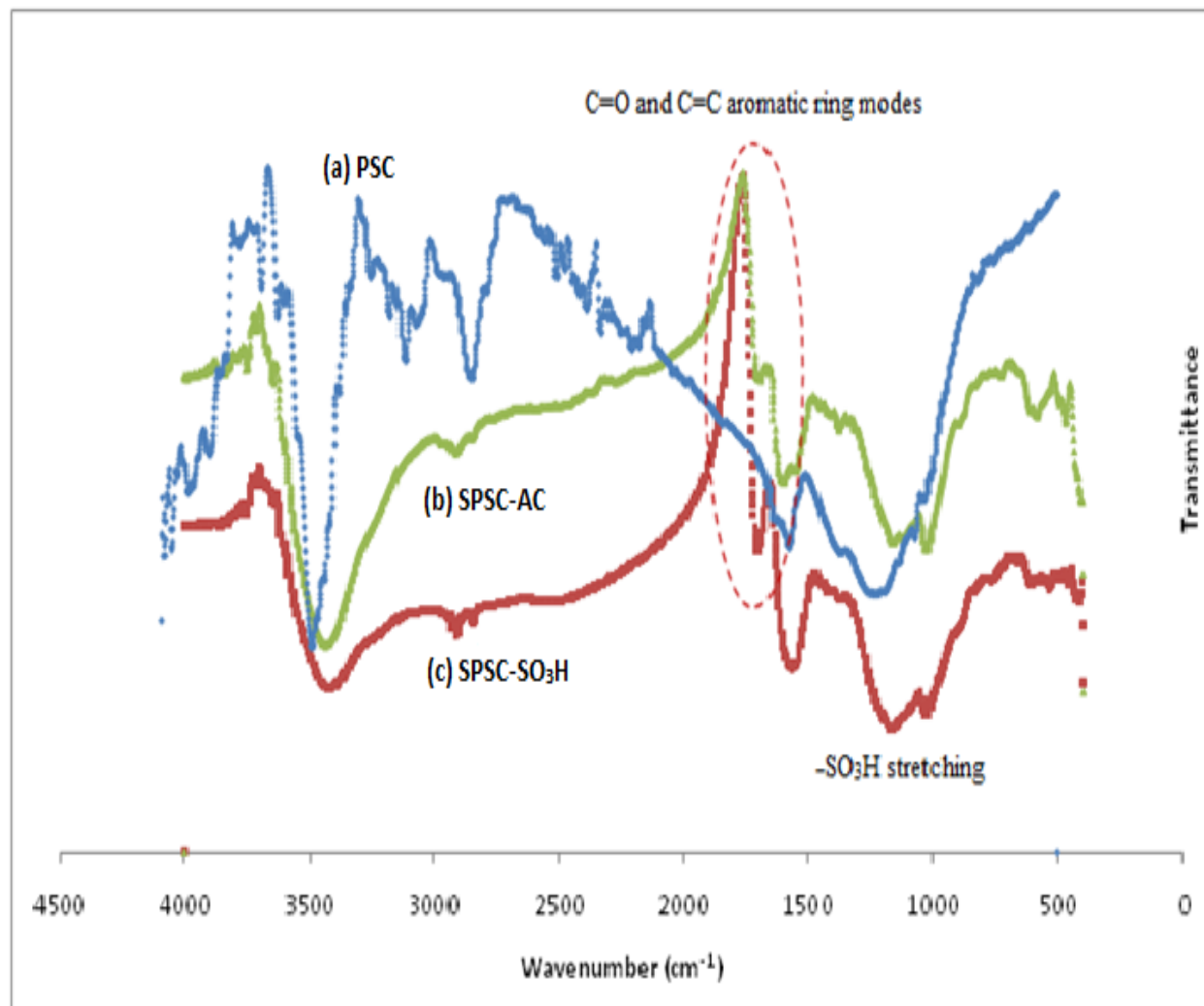
567



570

571 **Fig. 1**

572



573

574 **Fig. 2**

575

576

577

578

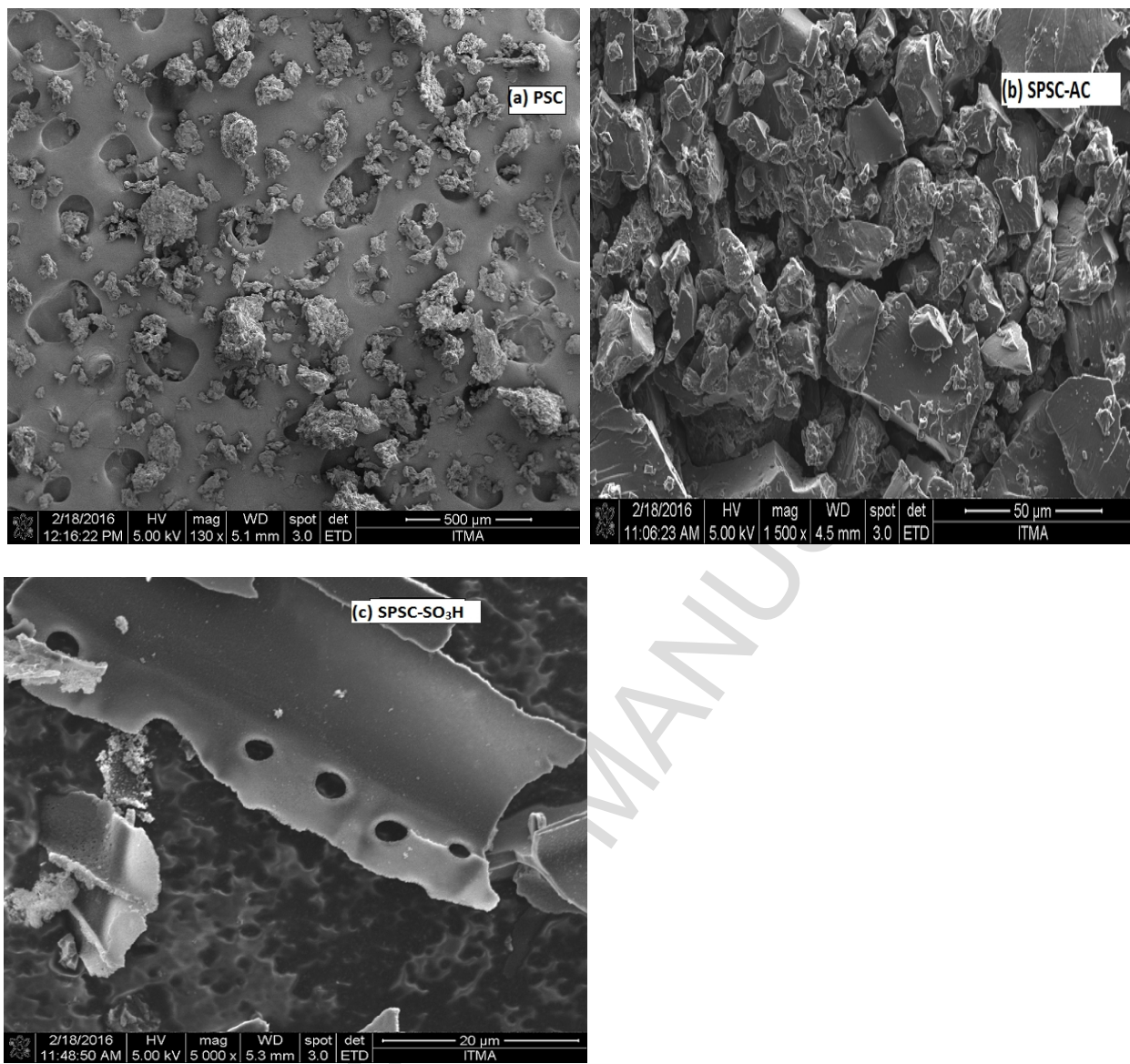
579

580

581

582

583



584

585

586

Fig. 3

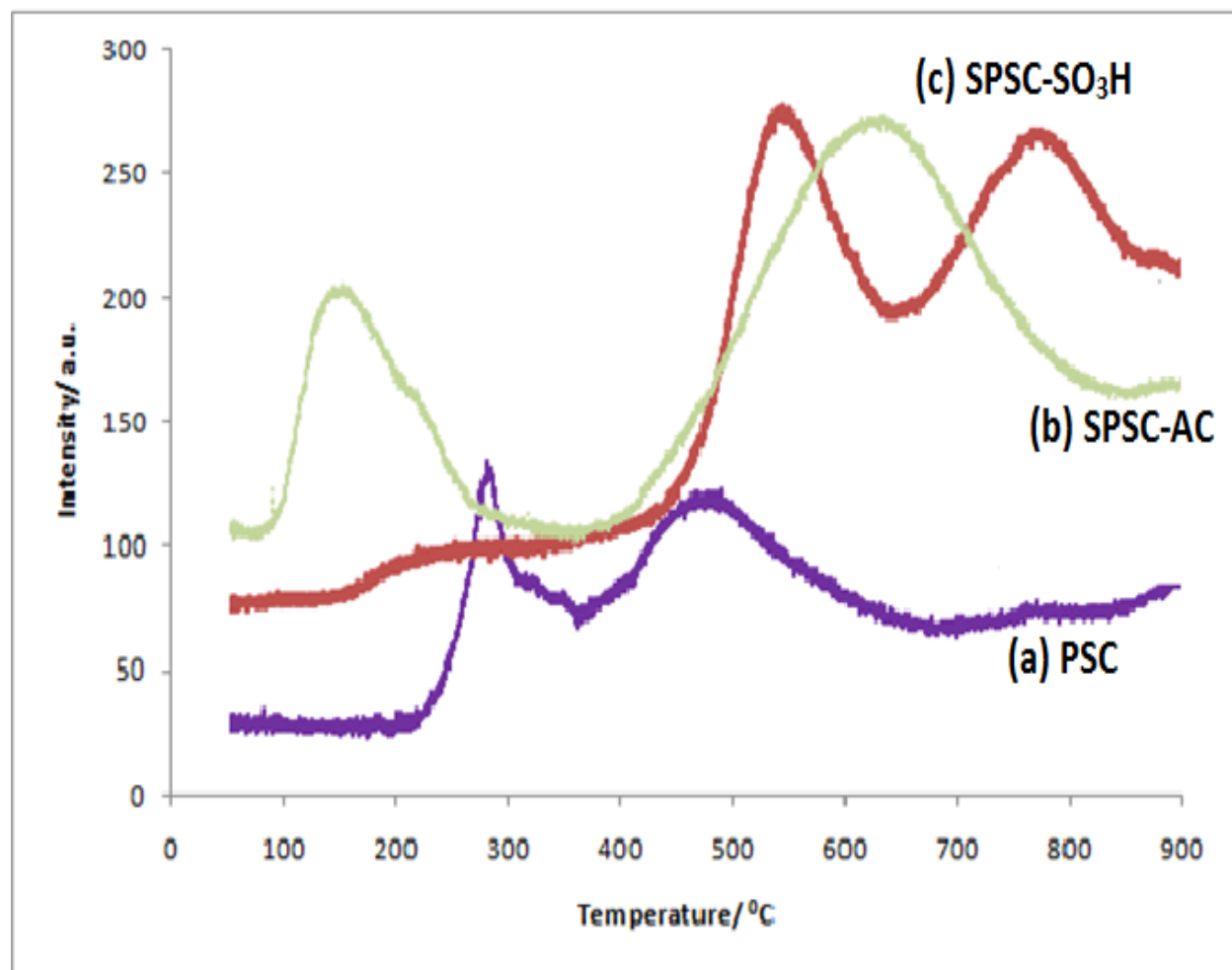
587

588

589

590

591



592
593 Fig. 4

594

595

596

597

598

599

600

601

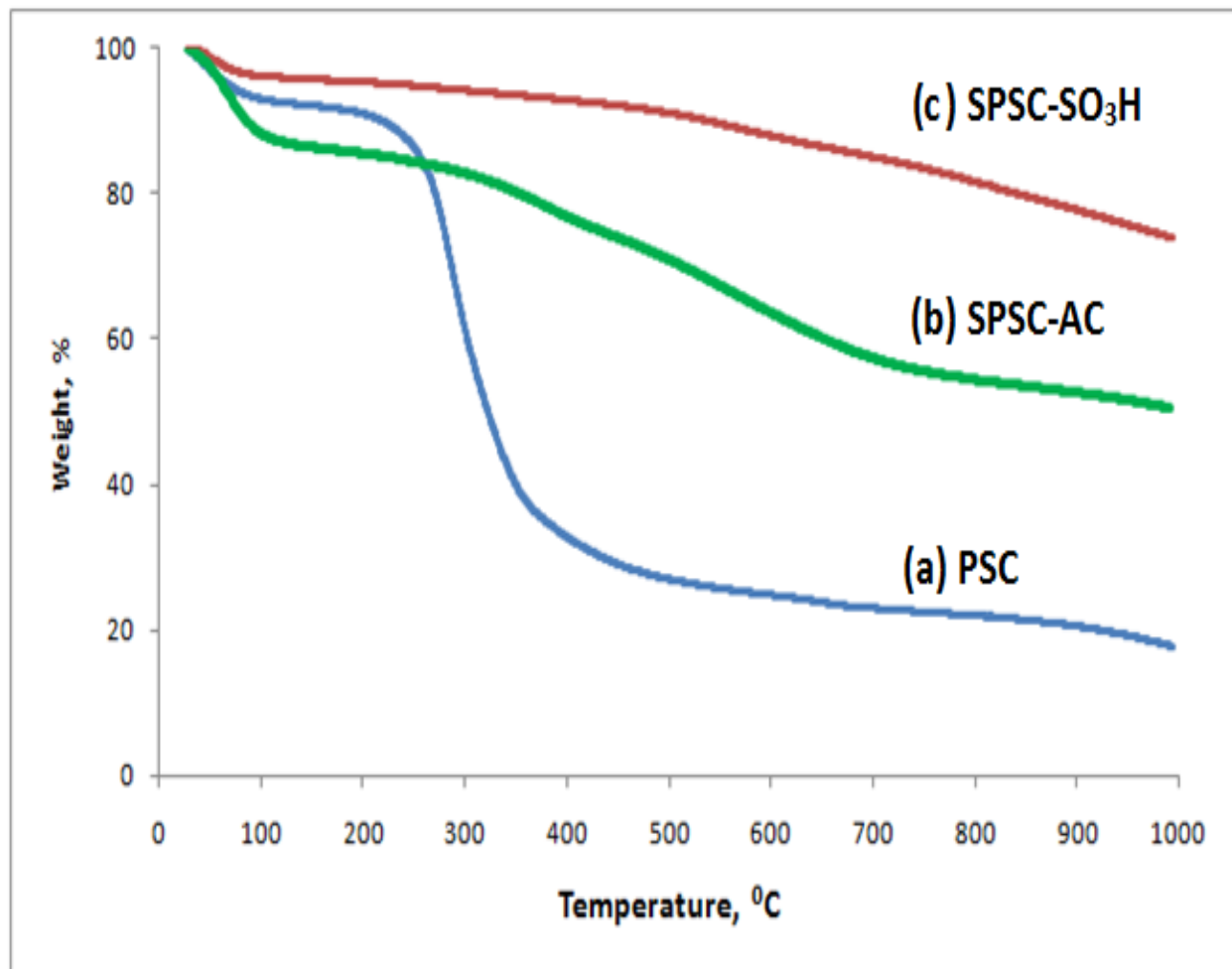
602

603

604

605

606



607
608 **Fig. 5**

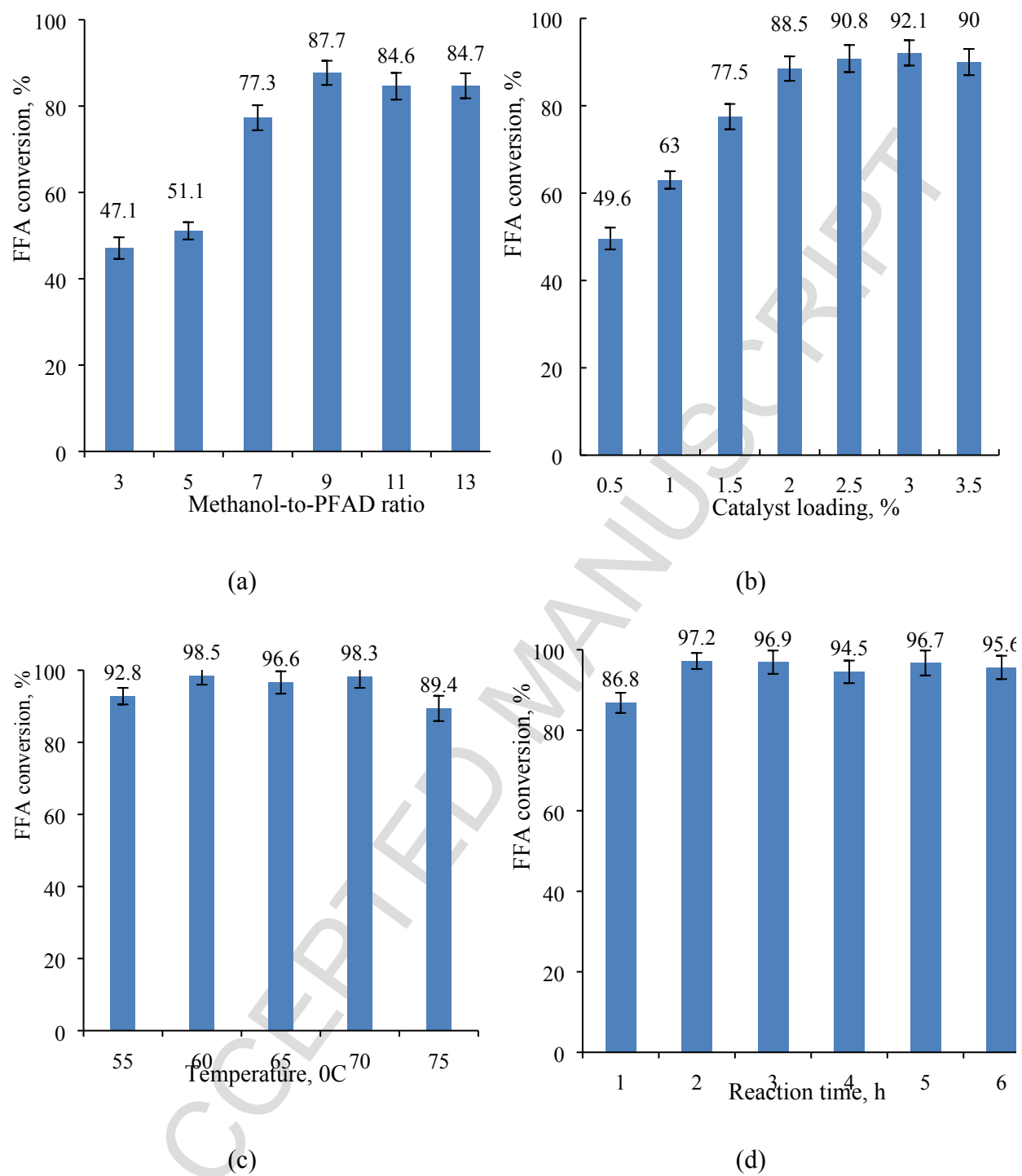
609

610

611

612

613

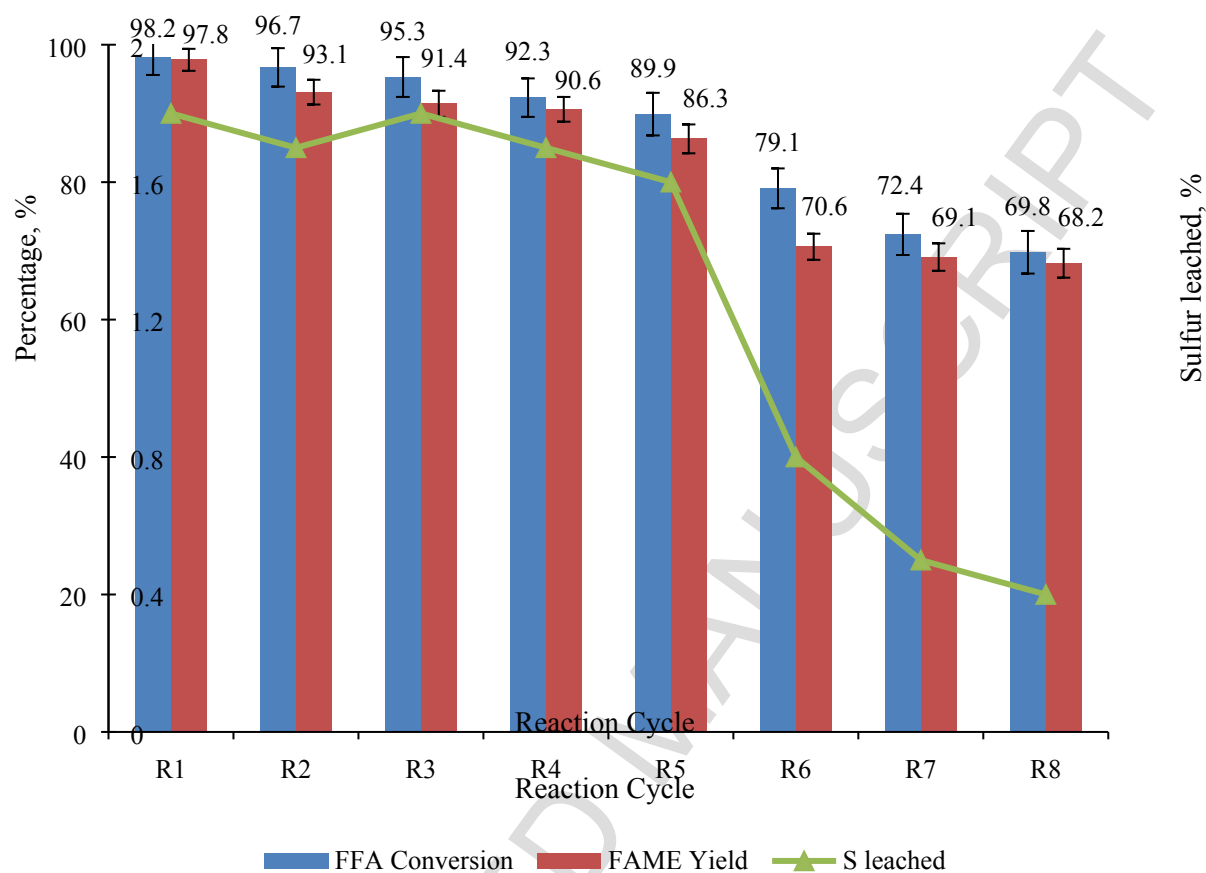


614

615 **Fig. 6**

616

617
618
619



620

621

Fig. 7

622

623

624

625

626

627

628

629

630

631

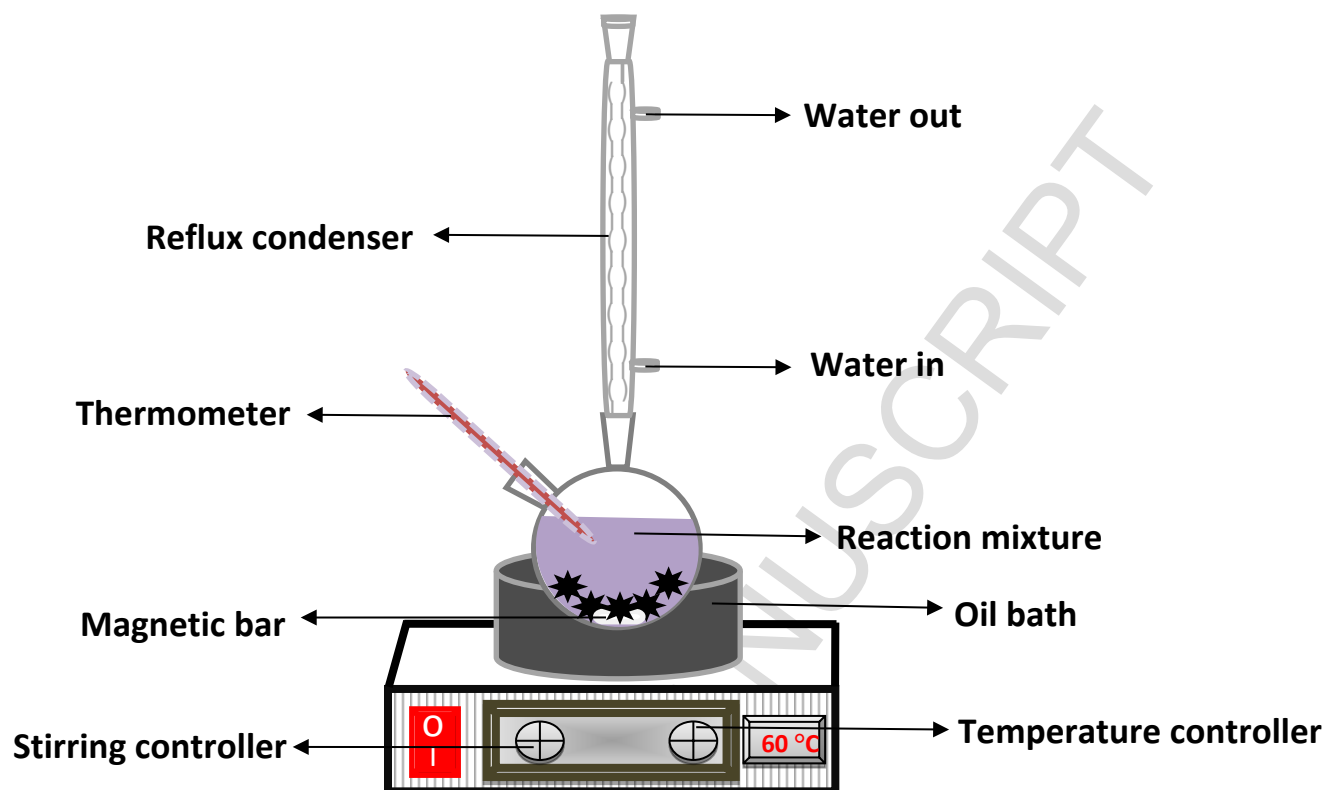
632

633

634

635

636



Scheme 1

664 **Table 1.** BET analysis of palm seed cake (PSC), palm seed cake- activated carbon (PSC-AC),
665 soaked palm seed cake – activated carbon (SPSC-AC) and sulfoanated soaked palm seed cake
666 (SPSC-SO₃H) catalyst

667

Sample	Specific surface area (m ² g ⁻¹)	Pore volume (cm ³ g ⁻¹)	Pore diameter (nm)
PSC	89.41	0.11	0.32
PSC-AC	107.05	0.15	0.95
SPSC-AC	658.34	1.18	5.09
SPSC-SO ₃ H	483.07	0.84	4.13

668

669

670

671

672

673

674

675

676

677

678

679

680

681

682

683

684

685

686

687 **Table 2.** Elemental and acid site density analysis of palm seed cake (PSC), soaked palm seed cake
 688 – activated carbon (SPSC-AC) and sulphonated soaked palm seed cake (SPSC-SO₃H) catalyst

689

Sample	C		O		S		Total acidity (mmol g ⁻¹)
	^a Weight (g)	^b Atomicity	^a Weight (g)	^b Atomicity	^a Weight (g)	^b Atomicity	
PSC	52.11	59.18	47.89	40.82	-	-	5.44
SPSC-AC	86.31	89.36	13.69	10.64	-	-	8.35
SPSC-SO ₃ H	66.65	73.65	30.19	25.02	3.16	1.31	12.08

690 ^aMeasured by using EDS analysis691 ^bMeasured by using CHNS elementally analysis

692

693

694

695